Influence of retinal ganglion cell nonlinearities on visual perception

Matthias H. Hennig[1,2] **and Florentin Wörgötter**[2]

[1] Department of Computing Science and Mathematics
University of Stirling
Stirling, FK9 4LA
UK
[2] Computational Neuroscience
Department of Psychology
University of Stirling
Stirling, FK9 4LA
UK

Key words: Motion Perception, Eye Movements, Fixation, Retinal Ganglion Cells, Model, Parvocellular System, Magnocellular System

Correspondence:
Matthias H. Hennig
Department of Computing Science and Mathematics
University of Stirling
Stirling
FK9 4LA
UK
Phone: +44 (0)1786 467448
FAX: +44 (0)1786 464551
Email: mhh@cs.stir.ac.uk

Stirling, 22 March 2005

Abstract

Commonly visual perception is thought to arise from the integrative properties of neuron populations in higher visual areas. Here, we describe two visual percepts showing that they have a direct correlate in the patterns of retinal ganglion cell activity. During fixation of a star-shaped stimulus, observers report a fading of complete wedges and an apparent splitting of stimulus lines. By means of a detailed retina model, we show that these percepts arise from motion caused by small fixational eye-movements. Both effects are visible in the population response of magnocellular (MC) ganglion cells, but not in that of the parvocellular (PC) stream. An analysis of single cell responses shows that the fading percept is a consequence of the transient nature of MC-cells leading to sectorial response adaptation. The splitting of lines originates from nonlinearities in the MC-cell receptive fields which also lead to frequency-doubling. We conclude that under these conditions visual perception is strongly influenced by magnocellular responses, possibly due to their transient nature. The results further indicate that receptive field nonlinearities enable magnocellular cells to encode perceptually relevant information invisible to a linear receptive field.

The process of visual perception is initiated by the responses of large populations of neurons in the visual system. Hence, usually individual response properties of a given neuron class cannot anymore be rediscovered at the perceptual level. Instead they disappear in higher visual areas due to integration over large populations of neurons and other mechanisms that facilitate the correct interpretation of a stimulus.

This is also the case for the properties of the two dominant visual processing streams, the parvo- or magnocellular systems are typically, which normally can not be perceptually discerned. These two streams originate in the retina from different populations of ganglion cells. In primates, the parvocellular stream is represented by linear PC-cells and the magnocellular stream by MC-cells, which show a substantial degree of spatiotemporal nonlinearity (Kaplan and Shapley, 1982; Benardete et al., 1992).

In this paper we will describe two novel visual illusions, which were studied using a model of the primate retina and confirmed in psychophysical experiments. The model, which is based on an earlier study of X- and Y-ganglion cells in the cat retina (Hennig et al., 2002), simulates responses of PC- and MC-cells. The simulated population activity shows that both illusions are induced by fixational eye movements and that the resulting percepts can be traced back to specific properties of the retinal magnocellular system.

Materials and Methods

Psychophysics

Two different experimental conditions were used. Experiment 1 was a qualitative survey. 35 naive subjects were shown a star shaped stimulus (Fig. 1A, on a CRT (n=22) or TFT (n=13) screen) during fixation of a red circle centered in the stimulus. They were asked to provide a verbal description of the percept.

In experiment 2, twelve subjects (10 naive) of both sexes with normal (5) or corrected (7) vision were shown a moving tilted cross or line (diameter $16.6°$, with the central $26'$ left blank, line width $1.3'$, presented on a Panasonic PanaSync S110 monitor at 91 Hz, background luminance was 5 cd/m^2, ambient luminance in the room was about 10 cd/m^2). Stimuli were viewed monocularly and a chin rest prevented head movements. Subjects were instructed to carefully fixate a dot ($3.9'$) in the center of the stimulus.

First, contrast detection thresholds were estimated using a static cross (mean threshold for all subjects $3.6\% \pm 1.6\%$). Then, either a tilted cross or a line was presented at six different contrast levels relative to the static threshold (2s presentation duration, during the first second, contrast was gradually increased to test level). During presentation, the stimulus was moved along one axis of the cross back and forth (maximum displacement $26'$). Until 0.5s after the presentation, the participants could report the stimulus type by key-press. We did not use a two-alternative forced choice procedure in order to avoid biasing of the responses. The experiment consisted of 120 randomly shuffled trials, the interval between trials was randomly varied between 1 s and 1.4 s. To ensure a constant performance, the subjects were given a break after 40 and 80 trials to relax the eyes (for details see supplementary material, Fig. S1).

Model

A computer model was used to simulate the parvocellular and magnocellular On-center channel in the primate retina under photopic conditions. Its structure is based on a previous model of Y- and X-cells of the cat retina (Hennig et al., 2002).

The activity of PC- and MC-cells was calculated in a 2-dimensional patch of hexagonally arranged neurons in the central 1.8 deg of the fovea. After convolution with a point spread function to simulate optical blurring, the stimulus is projected on a layer of 200x200 cones with an inter-cone separation of $0.55'$ (Curcio et al., 1987). Horizontal and bipolar cells receive synaptic input from photoreceptors. The horizontal cell layer was modeled as an electrically coupled syncytium and the activity is calculated at each site of synaptic contact to bipolar cells. On-center bipolar cells are inhibited by horizontal cells. Their density was assumed equal to the photoreceptor density (Wässle and Boycott, 1991). Two classes of bipolar cells were included, one sustained and one transient type. Transient bipolar cells receive inhibition from amacrine cells that leads to more transient responses. This inhibition is mediated by narrow-field amacrine cells, which are inhibited by wide-field amacrine cells. PC-cells receive input from sustained and MC-cells from transient bipolar cells (Boycott and Wässle, 1991; Roska and Werblin, 2001). Both types receive inhibition from wide field amacrine cells (Flores-Herr et al., 2001; Sinclair et al., 2004). The density of PC-cells was set equal to the photoreceptor density (Wässle and Boycott, 1991). For MC-cells, a ratio of 1:9 was assumed (Silveira and Perry, 1991). Further details about the model implementation are provided in the supplemental material.

Fixational eye movements include slow drift movements and the ocular microtremor. Drift movements were generated from a white noise power spectrum using the expression:

$$P(f) = \frac{A}{(1 + T_1 f)^2 * (1 + T_2 f)^2} \tag{1}$$

where $f[Hz]$ is the frequency, and $A = 3000$, $T_1 = 1.3$ and $T_2 = 0.1$ are constants, and horizontal and vertical components were generated independently. The power spectrum of the microtremor was modeled as Gaussian normal distribution with a peak at 80 Hz and standard deviation of 15 Hz (Bolger et al., 1999).

Stimulus was a static star at 100% contrast and high luminance. It had a diameter of $110'$ and consisted of 24 bars, each $2.86''$ wide.

Results

Characterization of the visual illusions

During careful fixation of the center of a star-shaped stimulus (Fig. 1A), one can observe two distinct effects. Typically, a fading or disappearing of lines or sectors of the stimulus occurs, which gradually changes its orientation and leads to apparent motion percepts. Additionally, often an apparent splitting of individual lines is visible. Both effects, in particular the latter, are short-lived and transient, and immediately disappear when fixation is lost.

In a qualitative assessment, we presented the star stimulus to naive subjects asking them to provide a verbal description of their percept during fixation. All subjects (n=35/35) reported that wedge-shaped sectors of this stimulus begin to fade; most often in two wedges opposite to each other. The location of the fading wedges rotates randomly, but not always all orientations are equally affected. Most observers reported that the fading predominantly occurs in an oblique axis, which may be a consequence of the oblique effect (Appelle, 1972), according to which horizontally and vertically oriented structures are better seen than oblique structures.

Additionally, 66% of the subjects (n=23/35) reported that lines appear to split or that they become denser, as if lines have been "added in between close to the center". Hence this illusion is less clear than the fading effect, which was confirmed by all observers. Observers also consistently reported that the percept is more short-lived than the line-fading.

Similar effects have been reported earlier for stimuli with a circular symmetry, such as for concentric circles by Purkinje and Helmholtz (Wade, 2003) and for the well-known MacKay Illusion (Pirenne et al., 1958). We noticed that the MacKay illusion induces a stronger splitting effect than the star shape we used. For this illusion, most observers (86%) reported that thin white lines suddenly split some of the wedges for a short moment in the middle.

In the following, we will first explain the retinal origin of these percepts by analysing population responses of the model retina. Then, the results of a psychophysical experiment, confirming a model prediction, are presented.

The representation of the illusions in modelled ganglion cell activity

The spatiotemporal activity during fixation of a star shaped stimulus (Fig. 1A) was simulated for populations of PC- and MC-cells. Small, involuntary eye-movements were included to simulate a physiological fixation condition (Fig. 1B).

Spatial activity patterns of the simulated ganglion cell populations are shown in Figure 1C-F. Snapshots were taken at the different times t_1 (Fig. 1C,E) and t_2 (Fig. 1D,F). Top panels (Fig. 1C,D) show PC-cell, those on the bottom (E,F) MC-cell responses (for movies of the activity patterns, see supplemental material, Fig. S3,S4).

The main effect of fixational eye movements is visible in Figure 1C-F. For both cell types, the bars of the stimulus cause a strong depolarization and the stimulus motion leads to a trailing hyperpolarization due to stimulation of the receptive field surrounds. Additionally, the activity of both cell types is reduced in two sectors, which are located along one axis of the stimulus. The orientation of this axis gradually changes as the direction of the eye movements change. This effect is much more pronounced in MC- than in PC-cells (compare E, F and C,D). In PC-cells, the membrane potential in the sectors with a reduced response is reduced by about 50% compared to the peak activity. In MC-cells, the responses in these sectors are reduced almost to resting potential.

How are eye-movements and fading-direction related? In the transition from the first snapshot at t_1 to the second at t_2, their direction has changed from approximately vertical to bottom-right (arrows in B). Thus, in both situations, fading occurs in sectors parallel to the eye-movement direction. In general, this type of on-axis fading occurs as soon as the axial eye-motion vector remains the same for more than 40 ms. The diagrams in panel G of show the activity of modeled

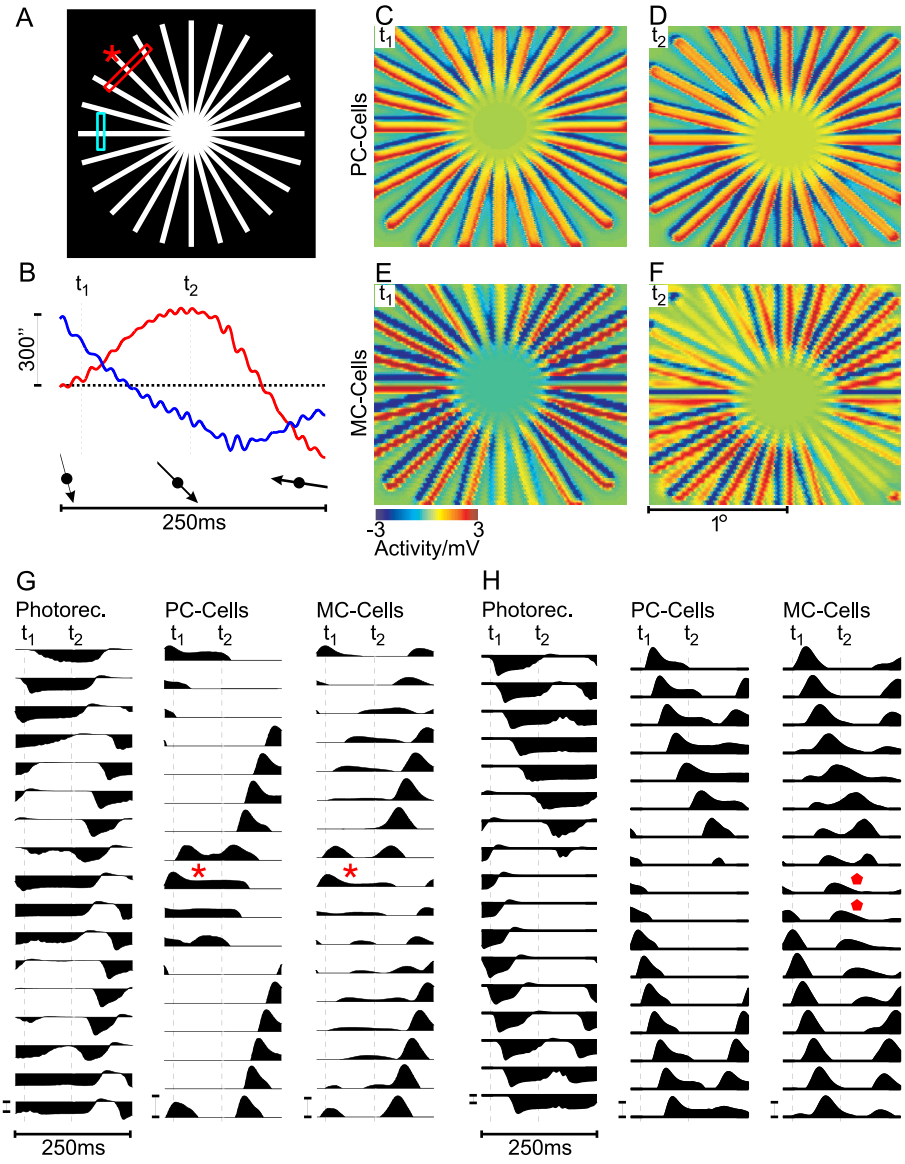

Figure 1: ⟶

photoreceptors, PC-cells and MC-cells for cells taken from the cross-section marked by the red bar in panel A. The receptive fields of the cells in the middle row (G, asterisks) are those that are stimulated by the marked line of the star-stimulus (asterisk in A). Motion of this line is approximately axial, thus the spatial stimulation of the corresponding receptive fields does not change much during this interval. As a consequence we find that the MC-cells more strongly adapt during this time than PC-cells, which leads to the observed activity drop in the MC-cell population.

Hence, these simulations suggest that the fading-percept may be an expression of the aperture problem at the level of retinal ganglion cells. The aperture problem results from the finite

Figure 1: Population activity of retinal ganglion cells during presentation of a star-shaped stimulus. A, Schematic drawing of the stimulus. Bars indicate where the single cell activity in panels G (red) and H (blue) was recorded. B, Simulated horizontal (red) and vertical (blue) eye movements. t_1 and t_2 indicate where the snapshots in C,D and E,F were taken. The relative combined motion direction is indicated by arrows. C-F, Spatial population activity of PC-cells (C and D) and MC-cells (E and F), taken at t_1 and t_2, as indicated in B. G, Activity of single photoreceptors, PC- and MC-cells at a location where axial fading is visible at time t_2 (red bar in A). The asterisks indicates where fading occurs in PC- and MC-cells (the location marked by an asterisk in A). H, as (G), but illustrating line splitting. Responses were taken from the region marked by a blue bar in A. Diamonds indicate where splitting is visible. In G and H, ganglion cell responses were clipped below resting potential to enhance visibility of the effects. Calibration bars correspond to 3 mV membrane potential.

dimension of the receptive field of a visual neuron. If an elongated stimulus is passing over a visual receptive field, the neuron will only respond to the motion component which is orthogonal to the orientation of the stimulus, because the axial components are invisible to the receptive field (Wallach, 1935; Hildreth and Koch, 1987). Hence, if adaption is present, on-axis movement will lead to activity drop in ganglion cells, like observed in the model. The susceptibility of MC-cells to this kind of aperture problem suggest that it should be possible to induce mispercepts in a low-contrast domain, where PC-cells are less responsive. The model specifically predicts that on-axis components of a moving star should remain invisible. Psychophysical results based on this prediction will be presented in the last chapter of this section.

The line-splitting effect is also visible in the simulated MC-cell population response (Fig. 1E,F). The snapshot from the MC-cell population taken at t_2 (Fig. 1F) shows that some lines display a spatially separated activity towards the periphery, which does not correspond to any part of the stimulus. Instead of the regular pattern of the stimulus, one finds pairs of depolarizing lines next to each other. This effect does not occur in the PC-cell population.

The comparison of the membrane potential traces details this observation (Fig. 1H). Photoreceptors and PC-cells show two moving, spatially separated activity peaks, which correspond to two lines of the stimulus. The same peaks are found in the MC-cells. Between both real peaks, however, MC-cell responses show a smaller additional activity peak (marked by the diamonds).

The model suggests that the splitting effect arises from the non-linear properties of a subgroup of MC-cells (MC_Y) which leads to frequency-doubling (Kaplan and Shapley, 1982; Benardete et al., 1992). Frequency doubling refers to the effect that certain MC-cells respond with a transient depolarization to a stimulus that reverses its contrast, but is otherwise spatially fully balanced over the receptive field (see the supplemental material, Fig. S5 for details).

What happens during fixation of the star stimulus? In this case fixational eye-movements may move two stimulus lines across opposite parts of a MC-cell receptive field. This creates competing on- and off-transients within the MC-receptive field, as shown in Figure 2: The photoreceptor responses in A correspond to a case where one bar leaves and the other enters the MC-receptive field. Panel B shows numerically differentiated photoreceptor responses, hence their transients, a simplification that in this form is not computed by the full model. However, this representation is sufficient to explain what happens. Since on- and off-transients are imbalanced, summation across the wide MC-receptive field (panel D) leads to remaining "ghost" activity at a location

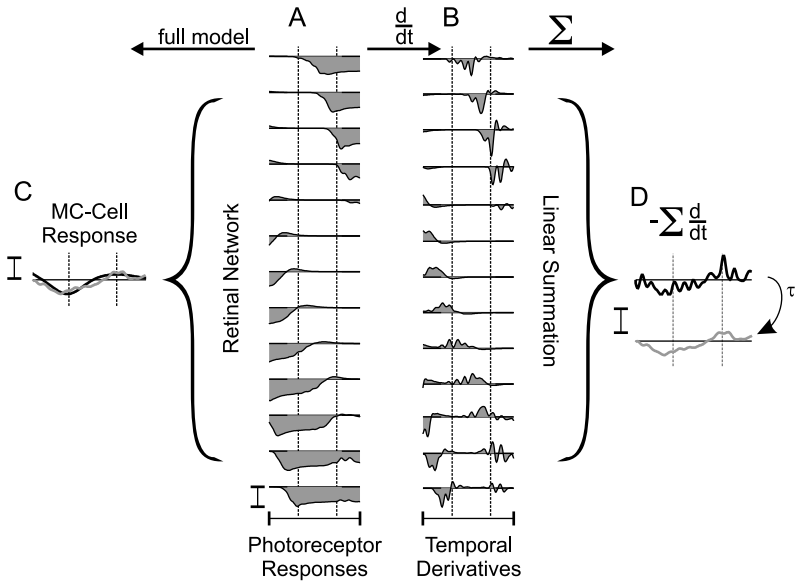

Figure 2: Frequency doubling in MC-cells causes the splitting percept. A, Simulated responses (150ms) of photoreceptors; B, their temporal derivatives calculated numerically and C, MC-cell responses to two lines of the star-shaped stimulus calculated with the full model. Brackets indicate the central $7'$ of the MC-cell receptive field. The response of the differentiated signals (B) summed across the bracket after inversion are shown in D (upper trace: raw data, lower trace: after low-pass filtering with $\tau = 4ms$). The low-pass filtered trace is also shown in C. Calibration bars indicate 5 mV.

without a physical stimulus. This response is superimposed, after scaling, inverting and applying a low-pass filter, onto the full model response in panel C. The good match indicates that in a first approximation line-splitting can be understood from the amplification and summing of differentiated photoreceptor responses. Consequentially, no line-splitting occurs in the model as soon as the activity of the nested amacrine circuit is blocked or when a linear photoreceptor model is used (data not shown).

Psychophysical correlates of the aperture problem

In a second, quantitative experiment we tested whether the fading percept can be induced. To this end an oblique cross (test condition) or line (control condition) was moved with an amplitude and velocity similar to slow drift movements, while subjects (N=12) maintained fixation. Using this procedure we wanted to actively induce a percept related to the aperture problem by biasing the stimulus motion on the retinal surface into one particular direction. Several contrast levels close to the static detection threshold were tested and observers had to report whether they saw a moving cross or a line.

In Figure 3A, B the results for two naive subjects in the test condition are shown. “Hit” refers to the detection of the cross, “error” to the detection of a line and “miss” to no recorded response. As expected, with increasing contrast both subjects had less misses and more hits. Close to the

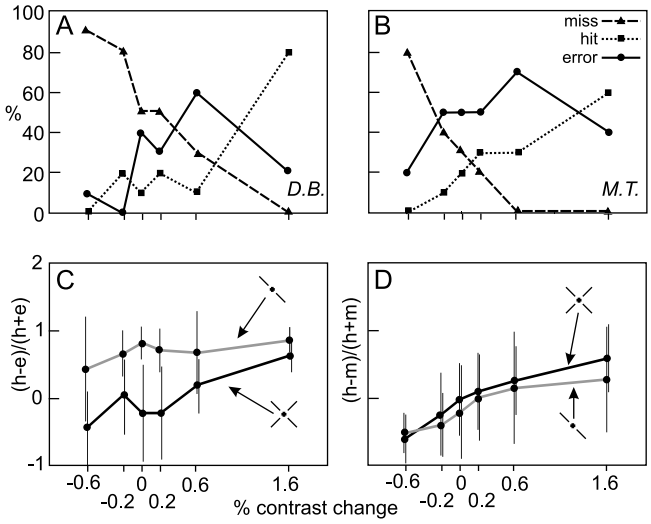

Figure 3: Line-fading can be induced by motion. A,B, Percentage of misses (triangles), hits (squares) and errors (circles) of two subjects who were presented with a moving oblique cross, plotted as a function of stimulus contrast relative to detection threshold (2.6% for both subjects). Correct responses refers to the reporting of a moving cross, false responses to the reporting of a moving line. C, Pooled data for 12 subjects as a function of contrast. Performance is given as relative difference of hits (h) and erroneous responses (e). Shown are results for the control condition, where an oblique line was shown (gray) and the test condition (black). Contrast values are expressed as in A,B. D, as C, but pooled relative difference of hits (h) and missed stimuli (m) for both cases.

static detection threshold however, only the orthogonally moving line remained visible, while the axially moving line could not be detected. Figure 3C,D shows the pooled performance of twelve subjects, comparing both conditions. Panel C shows that for the test stimulus, more often a line was reported at low contrasts than a cross (for all except the highest contrast: $p < 0.027$, one-tailed t-test). The strongest effect occurs at the estimated threshold contrast for each subject ($p < 0.0001$, one-tailed t-test). The comparison between hits and misses (D) for both conditions reveals no significant difference, indicating that the stimuli did not introduce any detection bias as such.

Thus, the visibility of a stimulus appears to be facilitated by motion, provided by fixational eye movements, as also suggested by Greschner et al. (2002), Hennig et al. (2002) and Rucci and Desbordes (2003). In particular, an orthogonal motion component is required, which may be a consequence of the aperture problem. Essentially these results confirm the predictions of the model.

Discussion

In this work, the origin of two visual percepts, both a consequence of fixational eye movements, has been traced back to specific properties of magnocellular ganglion cells. The results show that

both, perceived sectorial fading of a star and splitting of individual lines of the stimulus during precise fixation, are caused by the same receptive field properties that lead to transient responses and frequency-doubling in MC-cells.

Inevitably, a computational model of the retina can not provide a complete reproduction of its anatomy and physiology. Particularly the implementation of ganglion cell nonlinearities is critical as they are the basis for the results presented here, and we refer the reader to the supplemental material for further discussion. The accuracy of the model is however supported by the fact that the results we describe do not require a careful tuning of model parameters. Hence, we believe that the detail of the model is such that the associated membrane potential traces (Fig. 1 G,H) should be measurable in electrophysiological recordings.

Relations to existing psychophysical observations

Several impressive visual illusions exist which are elicited by retinal image motion due to eye- or head-movements, some of which were first described by Purkinje and Helmholtz (for a review, see Wade, 2003). These aesthetically appealing pictures, which have also influenced the arts ("Op-Art"), have been used to deduce possible neuronal mechanisms which underlie their perception. During fixation, observers report unstable flickering or apparent motion percepts, which can affect the image as a whole or parts of it.

The aperture problem has been discussed in conjunction with these illusions previously and models have been made to explain the Ouchi illusion (Mather, 2000; Fermüller et al., 2000) and others by means of simulated cortical motion detectors (Zanker, 2004; Zanker and Walker, 2004). Our study augments these findings by providing evidence for a retinal origin of these illusions. It is conceivable that the apparent motion elicited by these illusions requires at some point the activation of cortical motion detectors. Our results however indicate that this percept is not a consequence of specific properties of cortical motion detectors as such.

Implications for visual processing

It is commonly agreed that the finely grained activity from lower visual areas is integrated at higher levels of the processing hierarchy. In this study we have shown that this principle can be violated and that stimulus conditions exist, where the retinal activity pattern appears to directly match the visual percept. This finding suggests that higher processing stages may have contributed little to the processing and that specific properties of early visual responses can have direct perceptual correlates.

To our knowledge, the line splitting effect described here is the first perceptual correlate of the frequency doubling non-linearity of MC-cell receptive fields. [It should be noted that a clinically applied glaucoma test where the rapid contrast reversal of a grating leads to the precept of doubled spatial frequency is not a direct consequence of MC-cell frequency doubling (White et al., 2002).]

In principle, the splitting effect shows that MC-cells have the ability to encode spatiotemporal variations on a smaller spatial scale than their classical receptive field allows. It may therefore

be interesting to further investigate the influence of the MC-cell nonlinearities on the analysis of stimulus conditions relevant in natural scenes.

References

Appelle S (1972) Perception and discrimination as a function of stimulus orientation: the ”oblique effect” in man and animals. *Psychol Bull* 78:266–278.

Benardete EA, Kaplan E, Knight BW (1992) Contrast gain control in the primate retina: P cells are not X-like, some M cells are. *Vis Neurosci* 8:483–486.

Bolger C, Bojanic S, Sheahan NF, Coakley D, Malone JF (1999) Dominant frequency content of ocular microtremor from normal subjects. *Vision Res* 39:1911–1915.

Boycott BB, Wässle H (1991) Morphological classification of bipolar cells in the primate retina. *Eur J Neurosci* 3.

Curcio CA, Sloan KRJ, Packer O, Hendrickson AE, Kalina RE (1987) Distribution of cones in human and monkey retina: individual variability and radial asymmetry. *Science* 236:579–582.

Fermüller C, Pless R, Aloimonos Y (2000) The Ouchi illusion as an artifact of biased flow estimation. *Vision Res* 40:77–96.

Flores-Herr N, Protti DA, Wässle H (2001) Synaptic currents generating the inhibitory surround of ganglion cells in the mammalian retina. *J Neurosci* 21:4852–4863.

Greschner M, Bongard M, Rujan P, Ammermüller J (2002) Retinal ganglion cell synchronization by fixational eye movements improves feature estimation. *Nat Neurosci* 5:341–347.

Hennig MH, Kerscher NJ, Funke K, Wörgötter F (2002) Stochastic resonance in visual cortical neurons: does the eye-tremor actually improve visual acuity? *Neurocomputing* 44:115–120.

Hennig MH, Funke K, Wörgötter F (2002) The influence of different retinal subcircuits on the nonlinearity of ganglion cell behavior. *J Neurosci* 22:8726–8738.

Hildreth EC, Koch C (1987) The analysis of visual motion: from computational theory to neuronal mechanisms. *Annu Rev Neurosci* 10:477–533.

Kaplan E, Shapley RM (1982) X and Y cells in the lateral geniculate nucleus of macaque monkeys. *J Physiol* 330:125–143.

Mather G (2000) Integration biases in the Ouchi and other visual illusions. *Perception* 29:721–727.

Pirenne MH, Compbell FW, Robson JG, MacKay DM (1958) Moving visual images produced by regular stationary patterns. *Nature* 181:362–363.

Roska B, Werblin F (2001) Vertical interactions across ten parallel, stacked representations in the mammalian retina. *Nature* 410:583–587.

Rucci M, Desbordes G (2003) Contributions of fixational eye movements to the discrimination of briefly presented stimuli. *J Vis* 3:852–864.

Silveira LC, Perry VH (1991) The topography of magnocellular projecting ganglion cells (M-ganglion cells) in the primate retina. *Neuroscience* 40:217–237.

Sinclair JR, Jacobs AL, Nirenberg S (2004) Selective ablation of a class of amacrine cells alters spatial processing in the retina. *J Neurosci* 24:1459–1467.

Wade NJ (2003) Movements in art: from Rosso to Riley. *Perception* 32:1029–1036 Biography.

Wallach H (1935) Über visuell wahregenommene Bewegungrichtung. *Psychol Forsch* 20:325–380.

Wässle H, Boycott BB (1991) Functional architecture of the mammalian retina. *Physiol Rev* 71:447–479.

White AJ, Sun H, Swanson WH, Lee BB (2002) An examination of physiological mechanisms underlying the frequency-doubling illusion. *Invest Ophthalmol Vis Sci* 43:3590–3599.

Zanker JM (2004) Looking at Op Art from a computational viewpoint. *Spat Vis* 17:75–94.

Zanker JM, Walker R (2004) A new look at Op art: towards a simple explanation of illusory motion. *Naturwissenschaften* 91:149–156.

Influence of retinal ganglion cell nonlinearities on visual perception

Supplementary Material

Matthias H. Hennig[1,2] **and Florentin Wörgötter**[2]

[1] Department of Computing Science and Mathematics
University of Stirling
Stirling, FK9 4LA
UK
[2] Computational Neuroscience
Department of Psychology
University of Stirling
Stirling, FK9 4LA
UK

Stirling, 22 March 2005

Protocol for experiment 2

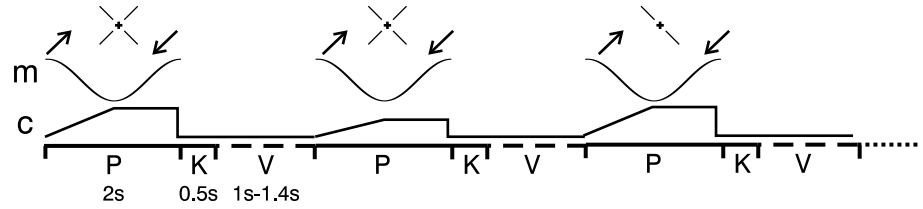

Figure S1: The protocol for the psychophysical experiment. During presentation (P, 2 s), the stimulus (shown on top) was moving in $+45^\circ$ direction with the waveform of a cosine (traces labeled m). During the first half cycle of the cosine, contrast was gradually increased to the test level (trace labeled c). During the presentation and for an additional interval (K), the subject's response was recorded. This was followed by a variable blank interval (V).

The model retina

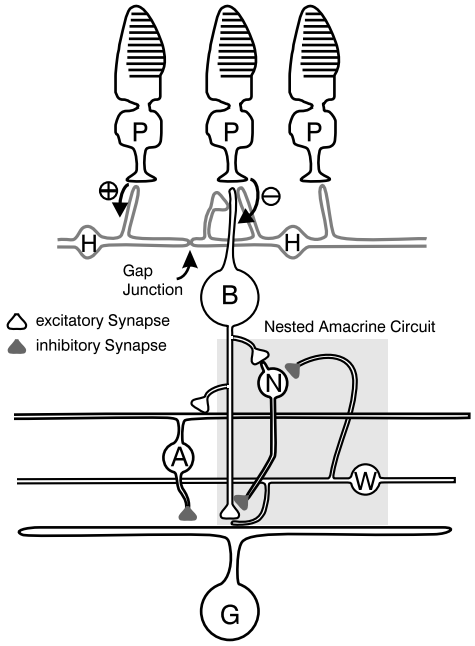

Figure S2: Structure of the model retina. Shown is the synaptic connectivity between the neuron classes included in the model. Photoreceptors (P) connect by excitatory synapses ($\oplus$) to horizontal cells (H) and sign-inverting synapses ($\ominus$) to On center bipolar cells (B). Horizontal cells (H) connect to On-center bipolar cells with sign-conserving synapses, mediating their receptive field surround. The receptive field of On-center ganglion cells (G) consists of excitatory input from On-center bipolar cells to the receptive center and inhibitory input from wide field amacrine cells (A) to the surround. The additional "nested amacrine circuit", consisting of narrow-field (N) and wide-field amacrine cells (W), is only included for MC-cells (shaded region, see Methods).

Figure S2 provides a summary of the synaptic connectivity of the model, as outlined in the main text. In the following, a more detailed description of the implementation of the individual cell classes will be given.

Neuron models and synaptic connectivity

Cone photoreceptor responses under photopic conditions were simulated by means of a state-variable description based on a model description of the photocurrent of macaque cones after a brief stimulation Schnapf et al. (1990). For an extensive description and discussion of this photoreceptor model, see (Hennig02a) (note there is a mistake in Eqn. 4 in this paper). The model consists of the following equations (parameters are given in Table 1):

$$\tau_{Casc}\frac{dS_i(t)}{dt} = S_{i-1}(t) - S_i(t), \tag{2}$$

$$\frac{d[cGMP](t)}{dt} = \underbrace{-\beta \cdot \Big([Ca^{2+}](t) - 1\Big)}_{\text{resynthesis}} \underbrace{-[PDE^*](t) \cdot [cGMP](t)}_{\text{stimulus induced}}, \tag{3}$$

$$\frac{d[Ca^{2+}](t)}{dt} = \underbrace{\gamma(1 + c \cdot ([cGMP](t) - 1))}_{\text{influx}} \underbrace{-\alpha \cdot [Ca^{2+}](t)}_{\text{efflux}}. \tag{4}$$

$$\frac{d[H](t)}{dt} = \left(\frac{1}{e^{(V_P(t) - A_H)S_H} + 1}\right) \cdot (1 - [H](t)) - \delta_H[H](t), \tag{5}$$

$$C_P \frac{dV_P(t)}{dt} = q_P \frac{d[Ca](t)}{dt} + q_I \frac{d[H](t)}{dt}, \tag{6}$$

All remaining neurons were implemented according to the membrane equation for a passive neural membrane with N synaptic inputs given by:

$$C\frac{dV(t)}{dt} = \left(\sum_{i=0}^{N} g_i(t) \cdot (V(t) - E_i)\right) + \frac{V_{rest} - V(t)}{R}, \tag{7}$$

where $g_i(t)$ is the conductance evoked by input i and E_i the corresponding reversal potential. The reversal potential for glutamatergic synapses was set to $0mV$, for GABAergic synapses to $-70mV$ and for glycinergic synapses to $-80mV$. $C = 100pF$ defines the membrane capacitance, $R = 100M\Omega$ the membrane resistance and $V_{rest} = -60mV$ the resting potential. Input conductances are linear functions of the presynaptic potential, which is expressed as $g_i(t) = V_{pre} \cdot 0.3nS/V$ for all cell types except for transient bipolar cells, where it was set to $g_{i,T}(t) = V_{pre} \cdot 0.4nS/V$.

Horizontal Cells The achromatic H1 horizontal cell was included in the model, which is held responsible for shaping the midget bipolar cell receptive field (Dacey et al., 2000; McMahon et al., 2004). The spatial decay of the activity of the syncytium was assumed to be Gaussian shaped. The standard deviation was set to four cone diameters, about the size of the midget cell receptive field surround in the fovea (Wässle et al., 1989). Horizontal cells in the model antagonize bipolar cells at a reversal potential of $E_{rev,inh} = -70mV$ Feigenspan et al. (1993), but the feedback pathway to cones was omitted (see also below).

Bipolar cells The model includes a sustained and a transient On-center bipolar cell type. All On-center bipolar cell types receive sign-inverting input from cones via the same metabotrophic glutamate receptor (mGluR6; Masu et al., 1995) and inhibition from horizontal cells. The transient bipolar cell type further receives GABAergic inhibition from narrow-field amacrine cells at their axon terminal (see below). This input is part of a circuit which leads to more transient responses.

Parameter	Eqns.	Description	Value
$S_i(t)$	1,2	Activity of the i-th low-pass filter stage (i=1..3, i=0: Stimulus). Emulates the initial amplification cascade.	
τ_{Casc}	1	Time constant of the low-pass filter.	$2ms$
$[cGMP](t)$	2,3	Concentration of hydrolyzed cGMP.	
β	2	Strength of the re-synthesis reaction of cGMP.	$1ms^{-1}$
$[Ca^{2+}](t)$	2,3	Intracellular concentration of Ca^{2+}.	
α, γ	3	Rates of efflux and influx of ions.	$0.4ms^{-1}$
c	3	Impact of $[cGMP]$ on the cation concentration.	$0.1ms^{-1}$
$[H](t)$	4	Hyperpolarization-activated I_h current.	
$V_P(t)$	4,5	Photovoltage.	
A_H	4	Activation of the h-current.	$-0.4V$
S_H	4	Slope of the activation function for the h-current.	$10V^{-1}$
δ_H	4	Rates of increase and decay of the ionic concentrations for the h-current.	$0.025ms^{-1}$
C_P	5	Membrane capacity.	$100pF$
q_P	5	Unit charge transported by the Ca^{2+} current.	$1 \cdot 10^{-9}C$
q_I	5	Unit charge transported by the I_h current.	$6 \cdot 10^{-9}C$

Table 1: Constants, variables and parameters of the photoreceptor model. It consists of the following stages: (1) three cascaded low-pass filters (Eqn. 1), (2) hydrolization of the second messenger cGMP (Eqn. 2) and Ca^{2+}-dependent re-synthesis, (3) in- and outflux of $Ca2+$ (Eqn. 3), (4) the hyperpolarization-activated I_h current (Bader and Bertrand, 1984; Demontis et al., 1999) (Eqn. 4) and the calculation of the photovoltage (Eqn. 5). Concentrations of second messengers and cations are calculated in dimensionless units relative to the boundaries $[0, 1]$ and the photovoltage is calculated in Volts.

Amacrine Cells GABAergic and glycinergic amacrine cells form a nested amacrine circuit that leads to truncation the input of MC-cells via the bipolar cell axon terminal (shaded region in Figure S2). A glycinergic wide-field amacrine cell receives excitatory input from the transient bipolar cell terminals and inhibitory input from GABAergic narrow field amacrine cells. Its receptive field is Gaussian shaped with a radius of $\sigma_C = 1.4'$. Narrow-field amacrine cells are excited by a single bipolar cell and receive inhibitory input from the nearest wide field amacrine cell. They cells provide inhibition to transient bipolar cells and wide field amacrine cells. It has been suggested that this specific circuit contributes to the transient responses of ganglion cells (Nirenberg and Meister, 1997; Roska et al., 1998).

A further GABAergic amacrine cell was implemented as an interneuron with a wide recep-

tive field (Gaussian radius $2.1'$ for those inhibiting PC-cells and $4.2'$ for MC-cells) that receives excitatory input from bipolar cells and inhibits ganglion cells (Flores-Herr et al., 2001; Sinclair et al., 2004).

Ganglion Cells The center input of ganglion cells is excitatory input from bipolar cells (transient for MC-cells and sustained for PC-cells). For PC-cells, the center is mediated by a single bipolar cell, and for MC-cells it was derived from a weighted Gaussian distribution with a width of $1.1'$.This is equivalent to a ratio of approximately 10:1 between the strongest and weakest inputs to a cells with dendritic field diameters in the range $4^{'}$-$5^{'}$ (Dacey and Petersen, 1992; Grünert et al., 1993; Cohen and Sterling, 1991).

An inhibitory surround is mediated by wide field amacrine cells with a receptive field of > 3.8 times the center input (Flores-Herr et al., 2001; Croner and Kaplan, 1995; Lee et al., 1998), which receive excitatory input from sustained (PC) or transient (MC) bipolar cells. For each cell type, the size of the centre was based on anatomical data, and it should be noted that the effective physiological receptive field is larger due to optical blurring and the influence of the presynaptic circuitry.

The proposed model for MC-cells is based on an earlier investigation of Y-cells in the cat (Hennig et al., 2002) and it shows a limited degree of contrast gain control and frequency doubling, as found in cat Y-cells (Enroth-Cugell and Robson, 1966). Experimental data indicates that the homology between PC/MC and X/Y-cells is partially valid (Kaplan and Shapley, 1982; Benardete et al., 1992). Therefore, the MC-cell in this study corresponds to the MC_Y-subtype as described by Benardete et al. (1992).

Optical Blurring Optical blurring was simulated by convolving the stimulus with a point spread function (PSF) given by Westheimer (1986) for the human fovea:

$$PSF(\rho) = 0.933 \cdot e^{-2.59 \cdot \rho^{1.36}} + 0.047 \cdot e^{-2.34 \cdot \rho^{1.74}}, \tag{8}$$

where ρ denotes the visual angle in minutes of arc.

Simulations The simulation software was developed in C++ and simulations were performed on a cluster of Intel x86/Linux computers. All numerical integration was performed in double precision using the second order Runge Kutta method.

Movies of the population activity of ganglion cells

Movie files moviePC.avi and movieMC.avi here, see
`http://www.cn.stir.ac.uk/~mhh1/Illusion`

Figure S3: The two movies show the spatiotemporal activity of a grid of simulated PC- and MC-cells (diameter $110'$) during stimulation with the star shaped stimulus (450 ms stimulus duration). The relative stimulus position is shown at the top of each frame (blue: horizontal displacement, green: vertical displacement). Below, the membrane potential of the ganglion cells is color coded for each neuron. The movies illustrate the main findings of the model study: (1) A substantial axial fading occurs in MC-cells and, much weaker, in PC-cells. It is visible along various directions, which are directly related to the motion of the stimulus on the retina. (2) Line-splitting, as described in this work, can be seen as additional yellow and red lines in the MC-cell population response, but not in that of PC-cells.

Movie files moviePC_rect.avi and movieMC_rect.avi here, see
`http://www.cn.stir.ac.uk/~mhh1/Illusion`

Figure S4: These movies show the data of Figure S1 after rectification of the membrane potential to simulate the spiking output of the ganglion cell populations. Rectification was achieved by calculating the spike rate $R(t)$ at each time step by the function $R(t) = 10 * (V_m + 2mV)^{1.4}$, where V_m is the membrane potential of the neuron (Mechler and Ringach, 2002).

Frequency doubling in MC-cells

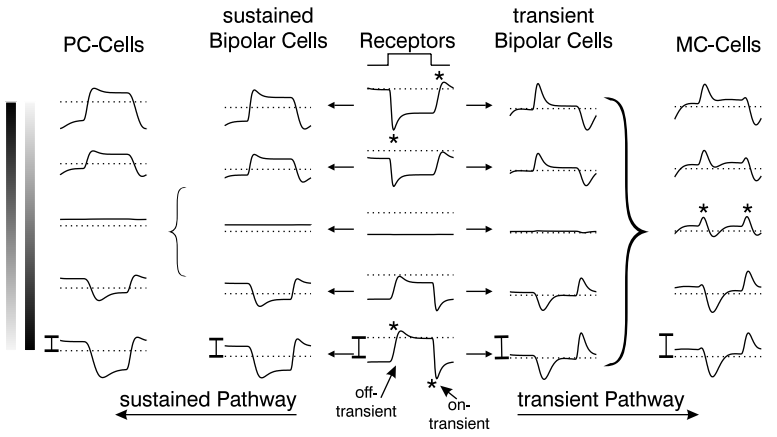

Figure S5: Illustration of frequency doubling responses in MC-cells during contrast reversal of a grating. The stimulus is indicated on the left (a grating at 11 cycles/degree). Simulated responses (200ms) of photoreceptors, sustained and transient bipolar cells and PC- and MC-cells are shown at five different spatial phases relative to the stimulus. For cells in the center, the net stimulation does not change during contrast reversal, but the MC-cell response shows phasic depolarizations at each reversal (asterisks). In photoreceptors one finds that a hyperpolarizing response to light onset produces a shaper and higher on-transient than the equivalent transient to light offset (off-transient), which is less strong and temporally more long lasting (asterisks). This asymmetry is amplified in transient bipolar cells via amacrine cells leading to a strong differential characteristic of the targeted MC-cells. Due to their smaller receptive fields and weaker asymmetries in bipolar cell responses, frequency doubling is not visible in PC-cells.

This discussion focuses on the nonlinearities in the simulated MC-cell receptive field, which are crucial for the results presented in the main text. The proposed model is based on an earlier investigation of Y-cells in the cat (Hennig et al., 2002). There, two main sources on nonlinearities were identified: the temporal response properties of simulated cone photoreceptors and a nested circuit of two amacrine cell types, which produces the transient responses of MC-cells. In summary, this model shows a limited degree of contrast gain control and frequency doubling, as originally described for cat Y-cells (Enroth-Cugell and Robson, 1966). As mentioned, the MC-cells in this study best correspond to the MC_Y-subtype (Benardete et al., 1992), and are therefore not a complete representation of the whole MC-population of the primate retina.

There is now strong evidence that multiple sites of origin for frequency doubling in ganglion cells exist. Specifically, in Y-like ganglion cells, temporal asymmetries in photoreceptors and bipolar cells seem to contribute as well as amacrine cells (Demb et al., 1999, 2001; Hennig et al., 2002). Figure S5 illustrates this for simulated MC-cells. In photoreceptors one finds that a hyperpolarizing response to light onset produces a shaper and higher on-transient than the equivalent transient to light offset (off-transient), which is less strong and slower (asterisks in Figure S5). This initially weak asymmetry is amplified in transient bipolar cells via amacrine cells leading to a strong differential characteristic of the targeted MC-cells. Due to their smaller

receptive fields and weaker asymmetries in bipolar cell responses, frequency doubling is not visible in PC-cells. In the model, several assumptions about retinal neurons were made which may affect the frequency-doubling nonlinearity.

Our previous results suggest that the present model is sufficient to explain frequency doubled responses in ganglion cells. Thus, while there may be other factors such as intrinsic mechanisms in bipolar cells, we assume that they are not critical at least in regard to frequency doubling. This also applies for a nonlinear relation between transmitter release and postsynaptic potential for excitatory synapses, which was assessed as a possible factor with the model. The main effect is a reduced hyperpolarization of the neuron due to reduced transmitter release by a presynaptic neuron. This is of importance for excitatory neurons and strong stimuli, as the driving force for hyperpolarization increases when the membrane potential is reduced. This drives the cell towards an extremely strong hyperpolarization. In this study however, the responses of the individual neurons were sufficiently weak so this effect was negligible and therefore not considered.

Generally, we found that the proposed amacrine circuit amplifies nonlinearities as a by-product of the inhibition that leads to transient responses. It was further observed that this may be the basis of a contrast gain control mechanism, as the difference between the activity of the wide and narrow-field amacrine provides a signal about local contrast, which was recently confirmed by an additional modelling study (Zaghloul and Boahen, 2004). Since the model contains no mechanism to increase the low cone contrast sensitivity in bipolar cells (as suggested by Snellman and Nawy, 2004), it operates only at higher contrast values $> 15\%$. Therefore, we believe our model provides an adequate description of MC-cell dynamics in the high contrast range studies in this paper.

In this study, a PC:MC cell ratio of 1:9 was assumed, which is in conflict with an estimate of 1:30 for the central retina by Dacey and Petersen (1992). As the coverage factor for MC-cells is > 1, this would result in substantially larger receptive fields. It is therefore important to consider how the expression of the nonlinearities, particularly frequency-doubling, changes for larger receptive fields. For simulated Y-cells we found that the magnitude of the second harmonic response remained constant for when the receptive field size was increased (Hennig et al., 2002), which suggests that the splitting effect we describe in the present paper should be visible even in MC-cells with wide receptive fields. On the other hand, it was shown in the same paper (Figure 10 there) that the lowest spatial frequency from which the second harmonic response dominates the first harmonic, i.e. when the cell behaves nonlinear and shows frequency doubling is related to the receptive field size (or more precisely, the cone convergence) by a power law. Thus, for small receptive fields, the second harmonic response is invisible because the contrast sensitivity has dropped due to optical blurring or other factors. Therefore, the receptive field proposed here could be a general prototype for nonlinear MC-cells in the primate retina.

In summary, our model is capable of reproducing relevant experimental data, which include both spatial and temporal response properties of primate PC and MC_Y ganglion cells. It should be noted that the effects described in the main text do not require careful tuning of model parameters, and that model parameters were adjusted by comparing model responses to published data on primate ganglion cells. Therefore, we expect that our findings should be directly testable experimentally in single cell recordings.

References

Bader CR, Bertrand D (1984) Effect of changes in intra- and extracellular sodium on the inward (anomalous) rectification in salamander photoreceptors. *J Physiol* 347:611–31.

Benardete EA, Kaplan E, Knight BW (1992) Contrast gain control in the primate retina: P cells are not X-like, some M cells are. *Vis Neurosci* 8:483–486.

Cohen E, Sterling P (1991) Microcircuitry related to the receptive field center of the On-Beta ganglion cell. *J Neurophysiol* 65:352–359.

Croner L, Kaplan E (1995) Receptive fields of P and M ganglion cells across the primate retina. *Vision Res* 35:7–24.

Dacey D, Packer OS, Diller L, Brainard D, Peterson B, Lee BB (2000) Center surround receptive field structure of cone bipolar cells in primate retina. *Vision Res* 40:1801–1811.

Dacey D, Petersen M (1992) Dendritic field size and morphology of midget and parasol ganglion cells in the human retina. *Proc Natl Acad Sci USA* 89:9666–9670.

Demb JB, Haarsma L, Freed MA, Sterling P (1999) Functional circuitry of the retinal ganglion cell's nonlinear receptive field. *J Neurosci* 19:9756–9767.

Demb JB, Zaghloul K, Haarsma L, Sterling P (2001) Bipolar cells contribute to nonlinear spatial summation in the brisk-transient (Y) ganglion cell in mammalian retina. *J Neurosci* 21:7447–7454.

Demontis GC, Longoni B, Barcaro U, Cervetto L (1999) Properties and functional roles of hyperpolarization-gated currents in guinea-pig retinal rods. *J Physiol* 515:813–828.

Enroth-Cugell C, Robson JG (1966) The contrast sensitivity of retinal ganglion cells of the cat. *J Physiol* 187:517–552.

Feigenspan A, Wässle H, Bormann J (1993) Pharmacology of GABA receptor Cl channels in rat retinal bipolar cells. *Nature* 361:159–161.

Flores-Herr N, Protti DA, Wässle H (2001) Synaptic currents generating the inhibitory surround of ganglion cells in the mammalian retina. *J Neurosci* 21:4852–4863.

Grünert U, Greferath U, Boycott BB, Wässle H (1993) Parasol (P alpha) ganglion-cells of the primate fovea: immunocytochemical staining with antibodies against $GABA_A$-receptors. *Vision Res* 33:1–14.

Hennig MH, Funke K, Wörgötter F (2002) The influence of different retinal subcircuits on the nonlinearity of ganglion cell behavior. *J Neurosci* 22:8726–8738.

Kaplan E, Shapley RM (1982) X and Y cells in the lateral geniculate nucleus of macaque monkeys. *J Physiol* 330:125–143.

Lee BB, Kremers J, Yeh T (1998) Receptive fields of primate retinal ganglion cells studied with a novel technique. *Vis Neurosci* 15:161–175.

Masu M, Iwakabe H, Tagawa Y, Miyoshi T, Yamashita M, Fukuda Y, Sasaki H, Hiroi K, Nakamura Y, Shigemoto R (1995) Specific deficit of the ON response in visual transmission by targeted disruption of the mGluR6 gene. *Cell* 80:757–765.

McMahon MJ, Packer OS, Dacey DM (2004) The classical receptive field surround of primate parasol ganglion cells is mediated primarily by a non-GABAergic pathway. *J Neurosci* 24:3736–3745.

Mechler F, Ringach DL (2002) On the classification of simple and complex cells. *Vision Res* 42:1017–1033.

Nirenberg S, Meister M (1997) The light response of retinal ganglion cells is truncated by a displaced amacrine circuit. *Neuron* 18:637–650.

Roska B, Nemeth E, Werblin FS (1998) Response to change is facilitated by a three-neuron disinhibitory pathway in the tiger salamander. *J Neurosci* 18:3451–3459.

Schnapf JL, Nunn BJ, Meister M, Baylor DA (1990) Visual transduction in cones of the monkey macaca fascicularis. *J Physiol* 427:681–713.

Sinclair JR, Jacobs AL, Nirenberg S (2004) Selective ablation of a class of amacrine cells alters spatial processing in the retina. *J Neurosci* 24:1459–1467.

Snellman J, Nawy S (2004) cGMP-dependent kinase regulates response sensitivity of the mouse on bipolar cell. *J Neurosci* 24:6621–6628.

Wässle H, Boycott BB, Röhrenbeck J (1989) Horizontal cells in the monkey retina: cone connections and dendritic network. *Eur J Neurosci* 1:421–435.

Westheimer G (1986) *Handbook of Perception and Human Performance*, Vol. 1, chapter The eye as an optical instrument John Wiley & Sons, New York.

Zaghloul KA, Boahen K (2004) Optic nerve signals in a neuromorphic chip I: Outer and inner retina models. *IEEE Trans Biomed Eng* 51:657–666.